Leukemia. Author manuscript; available in PMC 2021 March 22.

Published in final edited form as:
Leukemia. 2020 December 01; 34(12): 3206–3214. doi:10.1038/s41375-020-0816-y.

Mutational mechanisms of *EZH2* inactivation in myeloid neoplasms

Andrew Chase[1,2], **Joannah Score**[1,2], **Feng Lin**[1,2], **Catherine Bryant**[1,2], **Katherine Waghorn**[1,2], **Sarah Yapp**[1,2], **Gonzalo Carreno-Tarragona**[3], **Paula Aranaz**[4], **Aranzazu Villasante**[5,6], **Thomas Ernst**[7], **Nicholas C. P. Cross**[1,2]

[1]Faculty of Medicine, University of Southampton, Southampton, UK

[2]Wessex Regional Genetics Laboratory, Salisbury NHS Foundation Trust, Salisbury, UK

[3]Servicio de Hematología y Hemoterapia, Hospital Universitario 12 de Octubre, Madrid, Spain

[4]Centre for Nutrition Research, University of Navarra, Pamplona, Spain

[5]Institute for Bioengineering of Catalonia (IBEC), Barcelona, Spain

[6]Department of Electronics and Biomedical Engineering, University of Barcelona, Barcelona, Spain

[7]Abteilung Hämatologie/Onkologie, Klinik für Innere Medizin II, Universitätsklinikum Jena, Jena, Germany

Abstract

EZH2, a component of the polycomb repressive complex 2, catalyses the trimethylation of histone H3 lysine 27, a chromatin mark associated with transcriptional repression. *EZH2* loss-of-function mutations are seen in myeloid neoplasms and are associated with an adverse prognosis. Missense mutations in the SET/CXC domain abrogate catalytic activity as assessed by *in vitro* histone methylation assays, but missense mutations clustering in the conserved DI and DII regions retain activity. To understand the role of DI and DII mutations, we initially developed a cell-based histone methylation assay to test activity in a cellular context. Murine induced pluripotent stem cells lacking *EZH2* were transiently transfected with wild type or mutant *EZH2* (n=15) and any resulting histone methylation was measured by flow cytometry. All DI mutations (n=5) resulted in complete or partial loss of methylation activity whilst 5/6 DII mutations retained activity. Next, we assessed the possibility of splicing abnormalities induced by exon 8 mutations (encoding DII) using RT-PCR from primary patient samples and mini-gene assays. Exon 8 mutations resulted in skipping of exon 8 and an out-of-frame transcript. We have therefore shown that mutations within regions encoding EZH2 domains DI and DII are pathogenic by loss of function and exon skipping, respectively.

*Correspondence to: Andrew Chase, Wessex Regional Genetics Laboratory, Salisbury NHS Foundation Trust, Salisbury SP2 8BJ, UK, Tel: +(44) 1722 425193, Fax: +(44) 1722 338095, achase@soton.ac.uk.

Conflicts of interest

None of the authors have any relevant conflicts of interest or disclosures

Europe PMC Funders Author Manuscripts

Introduction

The last several years have seen enormous success in understanding the mutational landscape of myeloid malignancies although much remains to be understood about the functional and pathogenic consequences of these changes. Despite this new knowledge, discriminating mutations that are true drivers of disease from passenger mutations can still be problematic. For example, nonsense or frameshift mutations in epigenetic regulator genes such as *EZH2*, *TET2*, *ASXL1*, *DNMT3A* are generally clearly inactivating but the pathogenic consequences of missense mutations is usually uncertain. The increasing use of sequencing panels as part of the routine work up for patients with hematological malignancies frequently creates dilemmas with respect to diagnosis and prognosis when missense mutations are found.

EZH2 loss of function mutations are frequently seen in myeloid neoplasms and are associated with an adverse prognosis[1, 2]. EZH2 is a highly conserved component of the polycomb repressive complex 2 (PRC2), which catalyses the trimethylation of histone H3 lysine 27 (H3K27). We have previously shown that several missense mutations in the SET/CXC domains of EZH2 abrogate catalytic activity using an *in vitro* histone methylase transferase (HMT) assay[1], a finding that is further supported by more recent structural analysis[3–5]. Missense mutations outside the SET/CXC domains cluster in two regions known as DI and DII, suggesting that they are also likely to be functional. Unexpectedly, however, we found that DI and DII missense mutants retained catalytic activity using the *in vitro* HMT assay. We hypothesised that the cellular context, such as interaction with accessory proteins or chromatin, might also be relevant to the pathogenicity of DI and DII mutations. We therefore developed a cell-based H3K27 methylation (HM) assay, which revealed that DI mutations also abrogated HMT activity. DII mutants retained activity but further investigations revealed that they affected splicing, resulting in skipping of exon 8 and production of an out of frame *EZH2* mRNA.

Materials and Methods

Patient samples

Use of samples from patients diagnosed with myeloid neoplasms was approved by the National Research Ethics Service (UK) Committee South West and informed consent was obtained according to the principles of the Declaration of Helsinki. The source and diagnosis of all *EZH2* variants studied is given in Supplementary Table 1. Most of these variants were detected by Sanger sequencing, and thus variant allele frequencies are mostly not available.

Baculovirus expression, PRC2 purification and HMT assay

The expression of murine PRC2 components Ezh2, Eed and Suz12, purification and assay for histone methylation activity were performed as previously described[1].

Cell lines and expression constructs

The murine *Ezh2*-null induced pluripotent stem cell (iPS) line, *Ezh2* Δ/Δ clone 10[6], was kindly provided by Professor Manuel Serrano, Barcelona. Cells were grown on Geltrex

hESC-qualified Ready-To-Use (Thermo Fisher Scientific, Waltham, MA) in KnockOut DMEM (Thermo Fisher Scientific) supplemented with 1 mM sodium pyruvate, non-essential amino acids (1x), 2 mM L-glutamine, 100 U/ml Penicillin/Streptomycin, 15% Knockout serum replacement (all from Thermo Fisher Scientific), 2,000 U/ml ESGRO Leukemia Inhibitory Factor (Millipore/Merck, Darmstadt, Germany), 0.001% β2-mercaptoethanol (Sigma-Aldrich, St. Louis, MO). HEK293F (Thermo Fisher Scientific), grown as adherent cultures, and HeLa cells were grown in DMEM (Biosera) supplemented with 10% fetal calf serum. Mutations were introduced by site-directed mutagenesis into wild type *EZH2* in pCMV6-AN-HA (Origene, Rockville, MD, USA). WT and mutant *EZH2* were then transferred to pCAGIG[7] (a gift from Connie Cepko, Addgene plasmid #11159) which expresses GFP via an internal ribosome entry site.

Cell-based H3K27 methylation assay

Ezh2-null iPS cells were transfected with wild type or mutant pCAGIG-*EZH2* constructs by reverse transfection using Lipofectamine 2000 (Invitrogen, Carlsbad, CA). Briefly, Geltrex was applied to a 6-well plate and incubated at 37 °C for 10 minutes. Three μg of plasmid DNA and 9 μl of Lipofectamine 2000 were each separately diluted in 150 μl of Optimem (Thermo Fisher Scientific) then combined and incubated at room temperature for 5 minutes. The Geltrex was removed from the plate and the DNA/Lipofectamine mix was added in a total of 800 μl complete medium. After 10 minutes $1x10^6$ iPS cells were added per well in 200 μl medium. After 48 hours, the cells were harvested, fixed in 4% paraformaldehyde in PBS for 10 mins, washed twice in PBS then permeabilized in ice cold 90% methanol overnight. The cells were rehydrated with PBS, blocked in FACS buffer (0.3% BSA in PBS, 0.1% Proclin 300 (Sigma)) for 1 hour, stained with a primary antibody against H3K27me3 for one hour (Cell Signaling Technology, Danvers, MA; #9733) and a secondary Alexa Fluor 647 antibody (Cell Signaling Technology; #4414) for one hour. Levels of H3K27 methylation were then analysed by flow cytometry (Accuri C6; Becton Dickinson, Franklin Lakes, NJ). Transfected cells were selected by gating for GFP positivity, and H3K27 trimethylation levels were measured by median Alexa Fluor 647 intensity in GFP positive cells. H3K27me3 intensity measurements in pCAGIG-*EZH2*-mutant transfected cells were compared to intensity in pCAGIG vector and pCAGIG-*EZH2*-WT transfected cells which were normalised to 0 and 1 respectively. For all mutations, the assay was performed on two independent pCAGIG clones. For immunocytochemistry, cells were cytospun on to glass slides, fixed in 4% paraformaldehyde in phosphate buffered saline (PBS) and permeabilized in 0.1% Triton-X 100 in PBS. Cells were simultaneously stained for H3K27me3 and green fluorescent protein (Abcam, Cambridge, UK; ab13970) with secondary antibodies tagged with Dylight 594 (SeraCare Life Sciences, MA, USA; #042-09-15-06) and Alex Fluor 488 (Abcam; ab150173) respectively.

Splicing assays

Changes to splicing were assessed by RT-PCR on cDNA prepared from patient leukocytes (where available) and using the pSpliceExpress (pSE) minigene system[8]. RT-PCR used the following primers in exons flanking the exon with the mutation: reverse and forward primers of exon 5: 5’-CCAACACAAGTCATCCCATTAAA and 5’-GTCTCCATCATCATCATCGTCA; exon 6: 5’-TGGGAAAGTACACGGGGATAG and 5’-

TGCTGTGCCCTTATCTGGAA; exon 7: 5'-GAGTTGGTGAATGCCCTTGG and 5'-GCACTTACGATGTAGGAAGCA; exon 8: 5'-CGATGATGATGATGGAGAC and 5'-AGCTGTTTCTGTGTTCTTCCG and exon 14: 5'-TTGTGGGCTGCACACTGCAG and 5'-TTGGAGCCCCGCTGAATACT. To create the pSE construct, a genomic fragment containing *EZH2* exon 8 and portions of flanking introns 7 and 8 (hg19; chr7:148522642-148524184) was amplified from a bacterial artificial chromosome RP11-81I21 using primers containing the attB1 attB2 adapter recombination sites (Forward primer 5'- ggggacaagtttctacaaaaaagcaggctTGGAATCAATGTAGCGGATGAG; reverse primer 5'-ggggaccactttgtacaagaaagctgggtTGAGGTACAGCTGCTTGGG; *EZH2* specific sequences are in capitals) followed by clonase-mediated recombination into the pSE vector. Exon 8 mutations were introduced by site-directed mutagenesis. The pSE constructs containing wild type or mutated *EZH2* exon 8 were transiently transfected into HEK293F or HeLa cells with Lipofectamine 2000. At 48 hours, cells were lysed in Trizol (Thermo Fisher Scientific), RNA extracted, and cDNA synthesized according to standard protocols[9]. Primers within the pSliceExpress rat insulin genes which flank the introduced *EZH2* sequence were used to amplify the transcribed minigene (pSE-RTPCR_F: 5'-CAGCACCTTTGTGGTTCTCA; pSE-RTPCR-R: 5'-CAGTGCCAAGGTCTGAAGGT). Alternatively, PCR with a FAM labelled forward primer was used to allow quantification of band intensity after running on an ABI 3130 Genetic Analyzer (Applied Biosystems, Foster City, CA). Band intensity was measured using Genemarker (SoftGenetics, State College, PA) and ratio of intensity of spliced to unspliced PCR fragments was used as the measure of exon skipping.

Aberrant splicing was examined by western blotting using antibodies against N-terminal (Abcam; ab191080) and C-terminal EZH2 (Abcam; ab186006) with beta-actin (Sigma-Aldrich, MI, USA; A5441) as loading control.

In silico analysis

Variants were assessed for damage scores using Polyphen, GERP++, LRT, SIFT, Phylop, SiPhy, Mutation Assessor, Mutation Taster, FATHMM and PROVEAN from within Alissa Interpret (Agilent Technologies, Belgium) and for predicted splicing abnormalities using Ex-skip[10] (http://ex-skip.img.cas.cz/).

Results

Non-SET/CXC missense variants are clustered within domains DI and DII

EZH2 variants from the COSMIC database release 87 (https://cancer.sanger.ac.uk/cosmic; November 2018) were filtered to include only hematopoietic, non-lymphoid neoplasms and then further selected for missense variants, or nonsense and frameshift variants (Figure 1). Frameshift and nonsense variants showed little or no clustering within *EZH2*; this is expected since it is believed that loss of the C-terminal SET domain and its H3K27 methylation activity is the primary target of these mutations. In contrast, missense variants showed marked clustering within the DI, DII and SET/CXC regions.

In vitro and cell-based H3K27 methylation assays

Using an *in vitro* histone methylation transferase (HMT) assay we have previously shown that the SET/CXC mutants C576W, R690C and Y731D conferred loss or greatly reduced catalytic activity[1]. Using the same assay, we examined three more variants: F145C (region D1; from COSMIC data, mutations at F145 are recurrent, therefore likely to be pathogenic), Y244D (region DII; associated with chromosome 7 acquired uniparental disomy, therefore likely to be pathogenic) and D192N (between DI and DII, not recurrent, not associated with acquired uniparental disomy). We found no evidence for loss of methylation activity for any of these variants (Figure 2) raising the question as to whether these are true pathogenic mutants or non-pathogenic passenger mutations/constitutional variants.

The mechanism by which PRC2 is recruited to target genes is complex and incompletely understood. We hypothesised that the cellular context, such as interaction with accessory proteins or chromatin, might also be relevant to the pathogenicity of mutations. Such interactions would not be apparent using the *in vitro* HMT assay but might be in a cell-based assay. We therefore used an *Ezh2*-null murine iPS line which is negative for H3K27me3, but which becomes H3K27me3 positive when transfected with wild type *EZH2* (Figure 3A). In contrast to what we saw with the *in vitro* assay, the cell-based histone methylation (HM) assay showed F145C to be inactive, D192N to be active and Y244D to show greatly reduced activity. We then assessed additional *EZH2* mutants, identified from our patient samples or from the literature (Table 1), mainly falling within the DI and DII regions. Of the additional DI mutants assayed, 4/4 (L128F, P132S, M134K and K156E) showed complete loss of, or greatly reduced, methylation activity. The loss of histone methylation activity for two variants, L128F and M134K, was also confirmed by immunocytochemistry on cytospun iPS cells transiently transfected with wildtype or mutant *EZH2* (Supplementary Figure 1).

The six DII mutants tested were more variable with the five additional mutants showing partial loss of activity in one case (L252V) and no loss of activity in four cases (E249K, A255T, R288Q and R298L; Figure 3B). It is important to note that further work (described in the next section) showed DII variants to induce skipping of exon 8 causing a frameshift and loss of function. This pathogenic mechanism is not apparent in our cell-based histone methylation assay in which the *EZH2* mRNA is transcribed from a cDNA with no splicing of exons.

Two SET domain mutants (R690C and Y731D) showed complete loss of methylation activity, consistent with structural studies[3] and our previous HMT data[1].

Exon 8 mutations result in exon 8 skipping

Most DI variants show loss of methylation activity in the cell-based HM assay, but this was not the case for most DII variants. Although we cannot exclude the possibility that DII variants might interact with myeloid lineage-specific factors that are not expressed in iPS cells, we focused our analysis on the possibility that some variants might alter splicing as, for example, has been shown for many missense variants in *BRCA2*[11]. We examined splicing in primary samples with a range of variants by RT-PCR with primers within exons flanking the mutated exon. Single samples with variants in exons 5 (c.466A>G p.(L156E),

within DI), exon 6 (c.574G>A p.(D192N), between DI and DII), exon 7 (c.727A>C p.(K243Q), within DII) and exon 14 (c.1583G>A p.(C528Y), in the CXC domain) showed no altered splicing but four of four samples with exon 8 variants (c.754C>G, p.(L252V); c.763G>A, p.(A255T); c.863G>A, p.(R288Q); c.893G>T, p.(R298L)) showed a smaller band (Figure 4A).

RT-PCR products were cloned and sequenced. Exon 8 normally undergoes alternative splicing; a short 164 bp form is seen (e.g. in transcript NM_001203249) in most transcripts, but sometimes an additional 15 base pairs is included at the 3' end of the exon (e.g. NM_004456). In samples with the c.754C>G, c.763G>A and c.863G>A variants, two predominant PCR bands were seen which represented the shorter exon 8 variant plus a smaller band which completely lacked exon 8, resulting in a frameshift. Only a single small predominant band was seen with the c.893G>T variant which sequencing again showed to result from complete skipping of exon 8 (Figure 4C). This case was associated with chromosome 7 acquired uniparental disomy and the variant allele frequency by next generation sequencing was 0.96 which likely accounts for the lack of a normally spliced transcript. Material was available for western blotting in two exon 8 mutated samples, with variants c.754C>G and c.893G>T, and we found these to have reduced and complete loss of full length EZH2 respectively, consistent with the DNA and mRNA data (Supplementary Figure 2).

A faint PCR band could be seen in some control samples which appeared to be the same size as that showing skipping of exon 8 (Figure 4A). To explore this in more detail we used FAM-labelled RT-PCR to examine exon 8 skipping quantitatively (Figure 5A). This confirmed that samples with *EZH2* exon 8 mutations showed pronounced skipping of exon 8, whilst samples from other myeloid neoplasias showed very low-level skipping and control samples from healthy individuals showed almost no exon 8 skipping. All myeloid neoplasias without exon 8 mutations had Illumina Trusight myeloid panel sequencing data and, although numbers were small, we found no clear correlation between the background level of exon 8 skipping in myeloid neoplasias and the presence of splicing factor mutations (Figure 5a).

We used a minigene splicing assay to confirm these findings and to examine three additional *EZH2* exon 8 mutants (c.730T>G, c.745G>A and c.890A>G) for which cDNA was not available. In HEK293F cells, all seven mutants were found to result in increased skipping of exon 8 compared to that of wild type exon 8 (Figure 5b). The assay was repeated in HeLa cells which gave similar results to that in HEK293 cells (Figure 5C)

In silico analysis

We used several online tools to identify any features of exon 8 that might explain the difference in activity of DI and DII mutations or the propensity for skipping of exon 8. Ex-skip (http://ex-skip.img.cas.cz/) uses ESE (exonic splicing enhancer) and ESS (exonic splicing suppressor) data to predict the likelihood of a mutation inducing exon skipping compared to WT. We analysed all *EZH2* missense variants from COSMIC with Ex-skip and compared exon 8 variants with variants in all other exons (Supplementary Table 2). Although some of the exons contained too few variants to be informative, exon 8 contained

the highest proportion of variants predicted to induce skipping (7/11, 0.64) compared to all other exons (44/124, 0.35) (Chi-squared, p=0.065). Although this is consistent with the results of our splicing assays, Ex-skip was not able to identify all exon 8-skipping variants suggesting other factors not determined by the Ex-skip algorithm are operating. Because DI and DII mutations seem to be pathogenic by different mechanisms and are differentially inactive and active in the cell-based HM assay, we used damage scores to look for differences between the two groups of mutations. There was no clear pattern although SIFT and LRT Omega scores suggested exon 8 mutations were less damaging than DI mutations (Supplementary Table 3). The diagnoses of patients with DI and DII mutations were also examined (Supplementary Table 1) but no clear differences were found between the two groups.

Discussion

We have shown that *EZH2* missense mutations within regions DI and DII domain are pathogenic by loss of function and exon skipping, respectively. Although the precise mechanisms underlying these abnormalities remain to be elucidated, our findings expand our knowledge of pathogenic mutations outside the SET/CXC domain and provide functional tests by which new variants may be assessed.

Regions DI and DII were originally defined by high homology with Drosophila Enhancer of Zeste [E(z)][12] and recent detailed crystallographic studies have further refined their structure and function[5, 13]. PRC2 promotes spreading of H3K27 methylation to adjacent chromatin by positive feedback from binding of the PRC2 component EED to H3K27me3[13, 14]. Several domains within the N-terminal part of EZH2 encircle EED and contact the catalytic SET domain. Upon binding H3K27me3, a stimulation-responsive motif (SRM) within the N-terminal region of EZH2 undergoes a conformational change thereby stimulating SET domain activity. Functional work on several SRM mutants[5], including mutations at F145 and P132 also in our series, has shown they result in a loss of allosteric activation of methylation. The SRM extends from amino acids 128 to 159 and therefore occupies most of region DI and disruption of the SRM therefore likely accounts for most of the mutations seen in the region DI mutation hotspot. In our series of mutations, L128F, P132S, M134K, F145C and K156E lie within the SRM and the loss of function we have seen with these is consistent with what is now known about SRM function.

Two variants, D192N and A345T, lie outside of both the SRM and exon 8 and remained active in our cell-based HM assay. The COSMIC database describes mutations at D192N in three cases with endometrial cancer (reported as somatic)[15], myelodysplastic syndrome[16] and chronic myelomonocytic leukemia (somatic status not know, no associated chromosome 7 acquired uniparental disomy)[1]; and one case of D192Y in squamous cell carcinoma (reported as somatic)[17]. COSMIC describes two cases with A345T; one case of polycythemia vera for which somatic and acquired uniparental disomy status were not known[1] and a case of lung squamous cell carcinoma (The Cancer Genome Atlas, https://www.cancer.gov/tcga, sample name TCGA-33-6737-01) which is reported as somatic. Despite some of these cases being reported as acquired, *in silico* derived damage scores (Supplementary Table 3) largely indicate that they are benign or neutral and, together with

our cell-based HM results, it is most probable that these are passenger or benign constitutional variants rather than driver mutations.

Unexpectedly we found that mutations within region DII, which largely overlaps with exon 8, did not show loss of methylation activity in the cell-based HM assay but instead showed exon 8 skipping. Exceptions were Y244D and L252V which, in addition to inducing exon 8 skipping, also showed almost complete or partial loss of methylation activity, respectively. Y244D has the highest damage scores by several of the deleterious prediction tools (Phylop, Fathom, Provea, Polyphen; Supplementary table 3), consistent with the almost complete loss of methylation activity, indicating that other functional mechanisms, in addition to splicing deregulation, may operate in a subset of cases with exon 8 mutations.

Splicing prediction programs were not able to definitively predict the splicing changes we saw, although Ex-skip overall predicted that COSMIC exon 8 variants were more likely to induce skipping than non-exon 8 variants. The finding of a low level of exon 8 skipping in myeloid neoplasias without *EZH2* mutations but not healthy controls suggests the possibility of a degree of splicing deregulation in these cases. A high level of *EZH2* splicing deregulation involving multiple exons has also been described in myelodysplastic syndrome[18]. Although our samples numbers were too small to be conclusive this did not appear to be related to the presence of splicing factor mutations, which are known to be common in MDS and MDS/MPN.

Variant interpretation remains particularly challenging for tumour suppressor genes in which loss of function might occur via multiple mechanisms. As we and others have shown, structural studies and functional analysis remain the most reliable means of determining a variant's pathogenicity but are labor intensive. One hope is that saturation genome editing with a high-throughput functional readout as has been described for *BRCA1* [19], and development of more reliable *in silico* methodologies will improve our current piecemeal approach to variant interpretation.

Supplementary Material

Refer to Web version on PubMed Central for supplementary material.

Acknowledgements

We are grateful to Professor Manuel Serrano for providing us with the murine *Ezh2* knockout iPS cell line *Ezh2* Δ/Δ clone 10. This study was funded by Bloodwise Specialist Programme Grant nos. 13002 and 18007 to NCPC and AC.

References

1. Ernst T, Chase AJ, Score J, Hidalgo-Curtis CE, Bryant C, Jones AV, et al. Inactivating mutations of the histone methyltransferase gene EZH2 in myeloid disorders. Nat Genet. 2010; 42:722–726. [PubMed: 20601953]
2. Nikoloski G, Langemeijer SM, Kuiper RP, Knops R, Massop M, Tonnissen ER, et al. Somatic mutations of the histone methyltransferase gene EZH2 in myelodysplastic syndromes. Nat Genet. 2010; 42:665–667. [PubMed: 20601954]

3. Antonysamy S, Condon B, Druzina Z, Bonanno JB, Gheyi T, Zhang F, et al. Structural context of disease-associated mutations and putative mechanism of autoinhibition revealed by X-ray crystallographic analysis of the EZH2-SET domain. PLoS One. 2013; 8
4. Wu H, Zeng H, Dong A, Li F, He H, Senisterra G, et al. Structure of the catalytic domain of EZH2 reveals conformational plasticity in cofactor and substrate binding sites and explains oncogenic mutations. PLoS One. 2013; 8
5. Lee CH, Yu JR, Kumar S, Jin Y, LeRoy G, Bhanu N, et al. Allosteric Activation Dictates PRC2 Activity Independent of Its Recruitment to Chromatin. Mol Cell. 2018; 70:422–434. [PubMed: 29681499]
6. Villasante A, Piazzolla D, Li H, Gomez-Lopez G, Djabali M, Serrano M. Epigenetic regulation of Nanog expression by Ezh2 in pluripotent stem cells. Cell Cycle. 2011; 10:1488–1498. [PubMed: 21490431]
7. Matsuda T, Cepko CL. Electroporation and RNA interference in the rodent retina in vivo and in vitro. Proc Natl Acad Sci U S A. 2004; 101:16–22. [PubMed: 14603031]
8. Kishore S, Khanna A, Stamm S. Rapid generation of splicing reporters with pSpliceExpress. Gene. 2008; 427:104–110. [PubMed: 18930792]
9. Cross NC, Melo JV, Feng L, Goldman JM. An optimized multiplex polymerase chain reaction (PCR) for detection of BCR-ABL fusion mRNAs in haematological disorders. Leukemia. 1994; 8:186–189. [PubMed: 8289486]
10. Raponi M, Kralovicova J, Copson E, Divina P, Eccles D, Johnson P, et al. Prediction of single-nucleotide substitutions that result in exon skipping: identification of a splicing silencer in BRCA1 exon 6. Human mutation. 2011; 32:436–444. [PubMed: 21309043]
11. Fraile-Bethencourt E, Diez-Gomez B, Velasquez-Zapata V, Acedo A, Sanz DJ, Velasco EA. Functional classification of DNA variants by hybrid minigenes: Identification of 30 spliceogenic variants of BRCA2 exons 17 and 18. PLoS genetics. 2017; 13
12. Laible G, Wolf A, Dorn R, Reuter G, Nislow C, Lebersorger A, et al. Mammalian homologues of the Polycomb-group gene Enhancer of zeste mediate gene silencing in Drosophila heterochromatin and at S. cerevisiae telomeres. EMBO J. 1997; 16:3219–3232. [PubMed: 9214638]
13. Jiao L, Liu X. Structural basis of histone H3K27 trimethylation by an active polycomb repressive complex 2. Science. 2015; 350
14. Margueron R, Justin N, Ohno K, Sharpe ML, Son J, Drury WJ 3rd, et al. Role of the polycomb protein EED in the propagation of repressive histone marks. Nature. 2009; 461:762–767. [PubMed: 19767730]
15. Zehir A, Benayed R, Shah RH, Syed A, Middha S, Kim HR, et al. Mutational landscape of metastatic cancer revealed from prospective clinical sequencing of 10,000 patients. Nat Med. 2017; 23:703–713. [PubMed: 28481359]
16. Bartels S, Schipper E, Hasemeier B, Kreipe H, Lehmann U. Routine clinical mutation profiling using next generation sequencing and a customized gene panel improves diagnostic precision in myeloid neoplasms. Oncotarget. 2016; 7:30084–30093. [PubMed: 27029036]
17. Seiwert TY, Zuo Z, Keck MK, Khattri A, Pedamallu CS, Stricker T, et al. Integrative and comparative genomic analysis of HPV-positive and HPV-negative head and neck squamous cell carcinomas. Clin Cancer Res. 2015; 21:632–641. [PubMed: 25056374]
18. Shirahata-Adachi M, Iriyama C, Tomita A, Suzuki Y, Shimada K, Kiyoi H. Altered EZH2 splicing and expression is associated with impaired histone H3 lysine 27 tri-Methylation in myelodysplastic syndrome. Leuk Res. 2017; 63:90–97. [PubMed: 29127861]
19. Findlay GM, Daza RM, Martin B, Zhang MD, Leith AP, Gasperini M, et al. Accurate classification of BRCA1 variants with saturation genome editing. Nature. 2018; 562:217–222. [PubMed: 30209399]
20. Bejar R, Stevenson K, Abdel-Wahab O, Galili N, Nilsson B, Garcia-Manero G, et al. Clinical effect of point mutations in myelodysplastic syndromes. N Engl J Med. 2011; 30:2496–2506.
21. Grossmann V, Kohlmann A, Eder C, Haferlach C, Kern W, Cross NC, et al. Molecular profiling of chronic myelomonocytic leukemia reveals diverse mutations in >80% of patients with TET2 and EZH2 being of high prognostic relevance. Leukemia. 2011; 25:877–879. [PubMed: 21339759]

22. Score J, Hidalgo-Curtis C, Jones AV, Winkelmann N, Skinner A, Ward D, et al. Inactivation of polycomb repressive complex 2 components in myeloproliferative and myelodysplastic/myeloproliferative neoplasms. Blood. 2012; 119:1208–1213. [PubMed: 22053108]

Europe PMC Funders Author Manuscripts

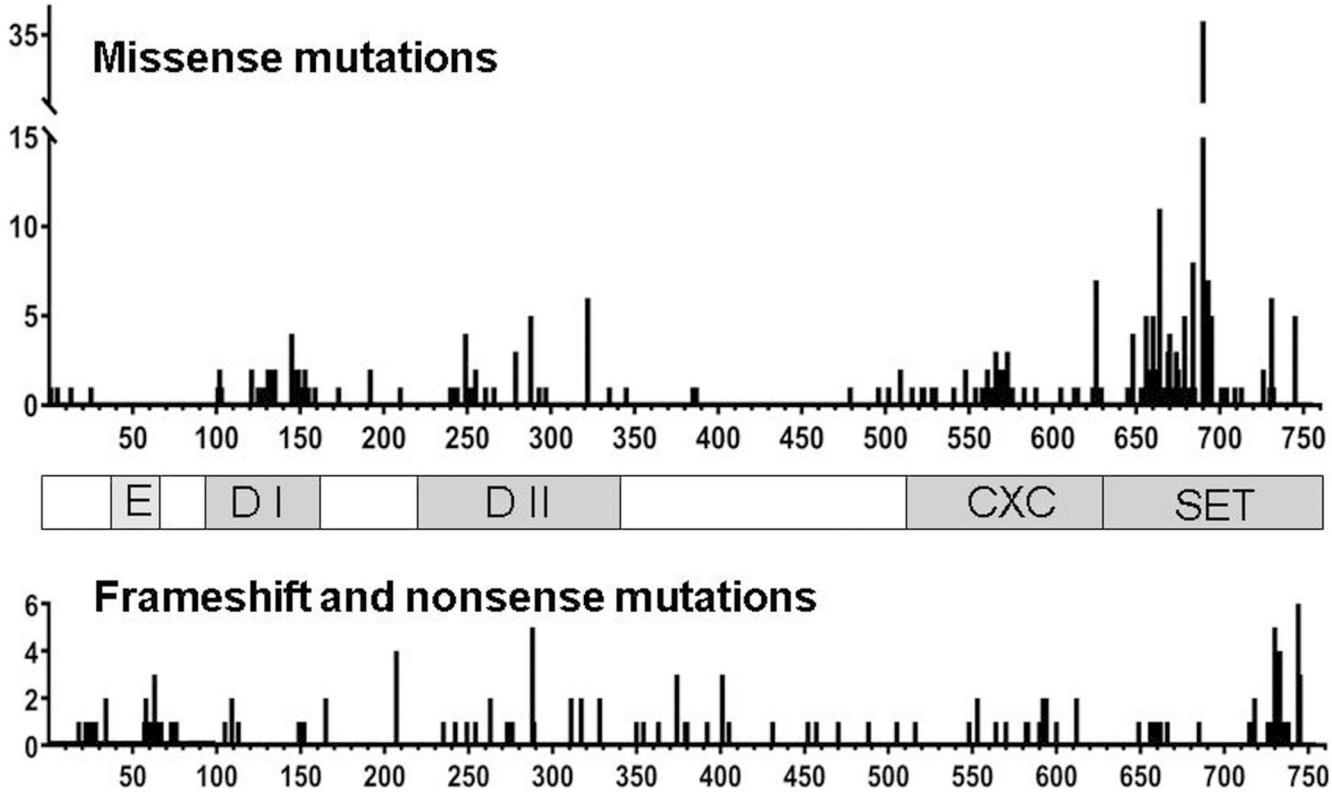

Figure 1.

EZH2 mutations from COSMIC, selected for non-lymphoid hematopoietic neoplasms, showing amino acid numbering. Missense mutations show clustering in the DI, DII and CXC/SET regions. Very little clustering is seen with frameshift and nonsense mutations.

Europe PMC Funders Author Manuscripts

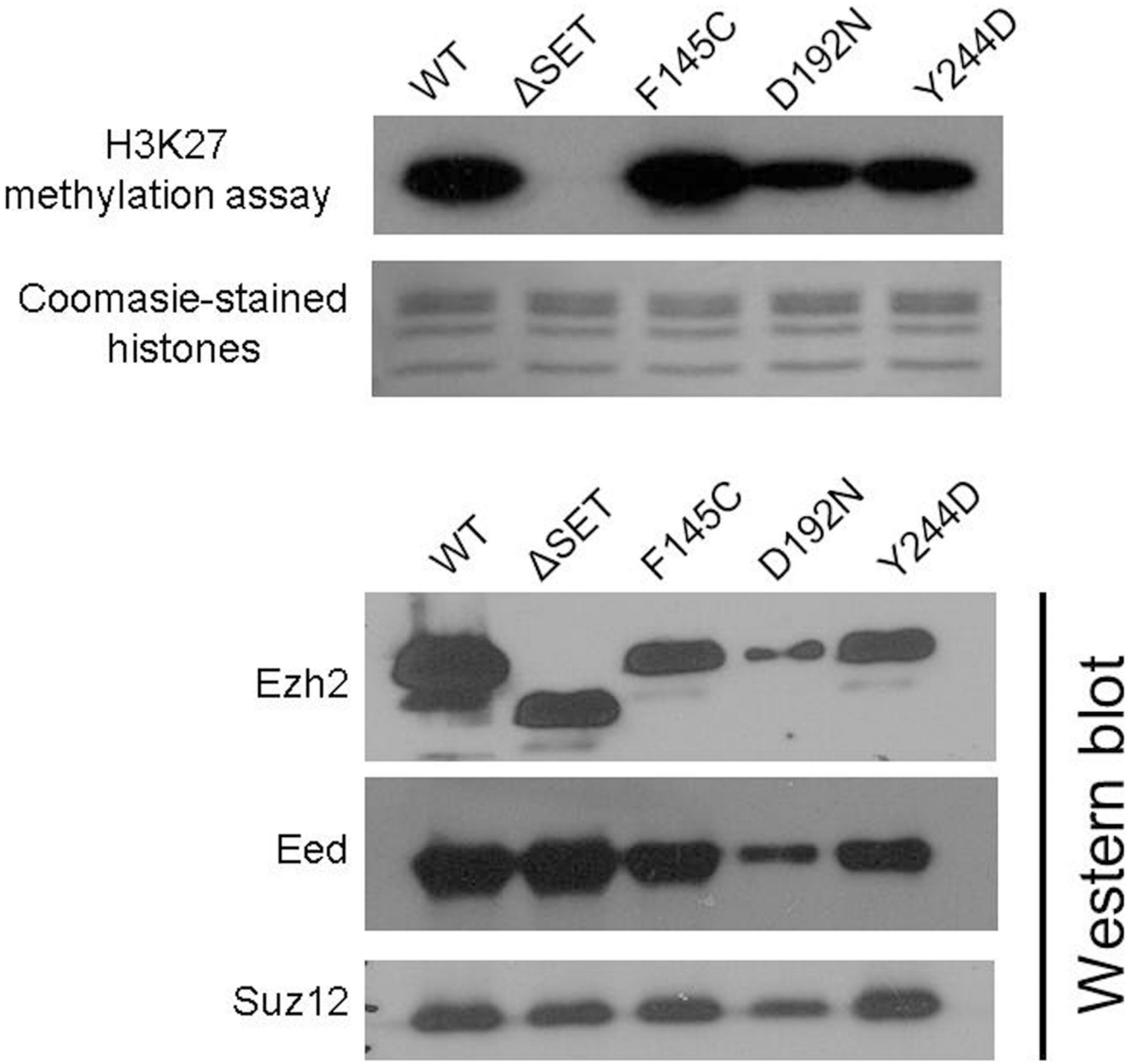

Figure 2.

In vitro histone methylation assay of baculovirus expressed components shows retained activity of Ezh2-mutant PRC2 complexes for the three variants tested. WT (wild type) and ΔSET (SET domain deletion mutant) are positive and negative Ezh2 controls, respectively; F145C, D192N and Y244D are Ezh2 variants that lie in DI, between DI and DII, and in DII regions respectively. The upper panel (Coomassie stained histones) shows equal loading of histone substrates in each reaction. In the lower panels, Western blots with antibodies against Eed, Suz12 and Ezh2 confirm the presence of all three PRC2 components.

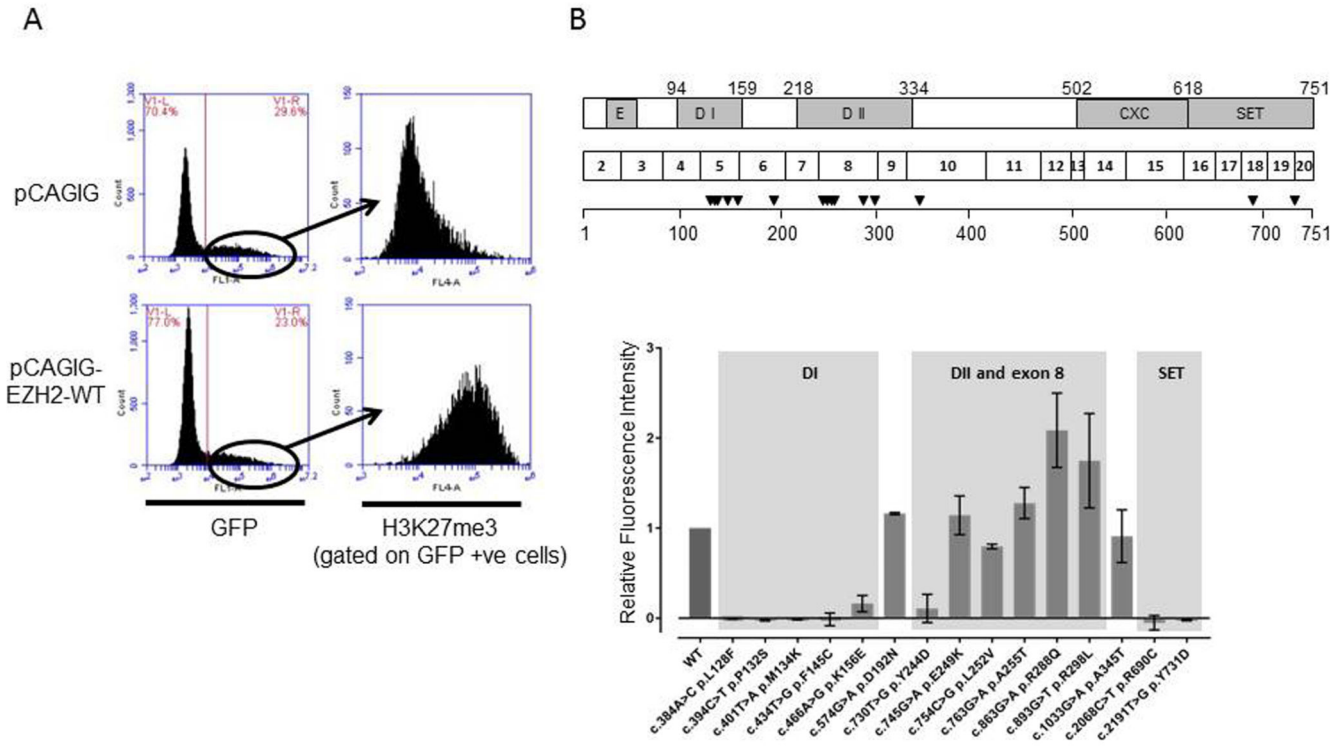

Figure 3.

Assessment of methylation activity of *EZH2* mutations methylation activity by flow cytometry. (A) At 48 hours after transfection with pCAGIG-EZH2-IRES-GFP, Ezh2-null iPS cells were stained for H3K27me3. Transfected cells, identified by GFP positivity, became H3K27me3 positive when transfected with wild type EZH2 (low panels) but not with the vector control (upper panels). (B) EZH2 constructs with a range of mutations (amino acid positions are shown in upper panel aligned against EZH2 exons and domains) were transfected into Ezh2-null iPS cells. Intensity of fluorescence was normalised to 0 and 1 for vector only and wild type EZH2 transfected cells respectively.

Europe PMC Funders Author Manuscripts

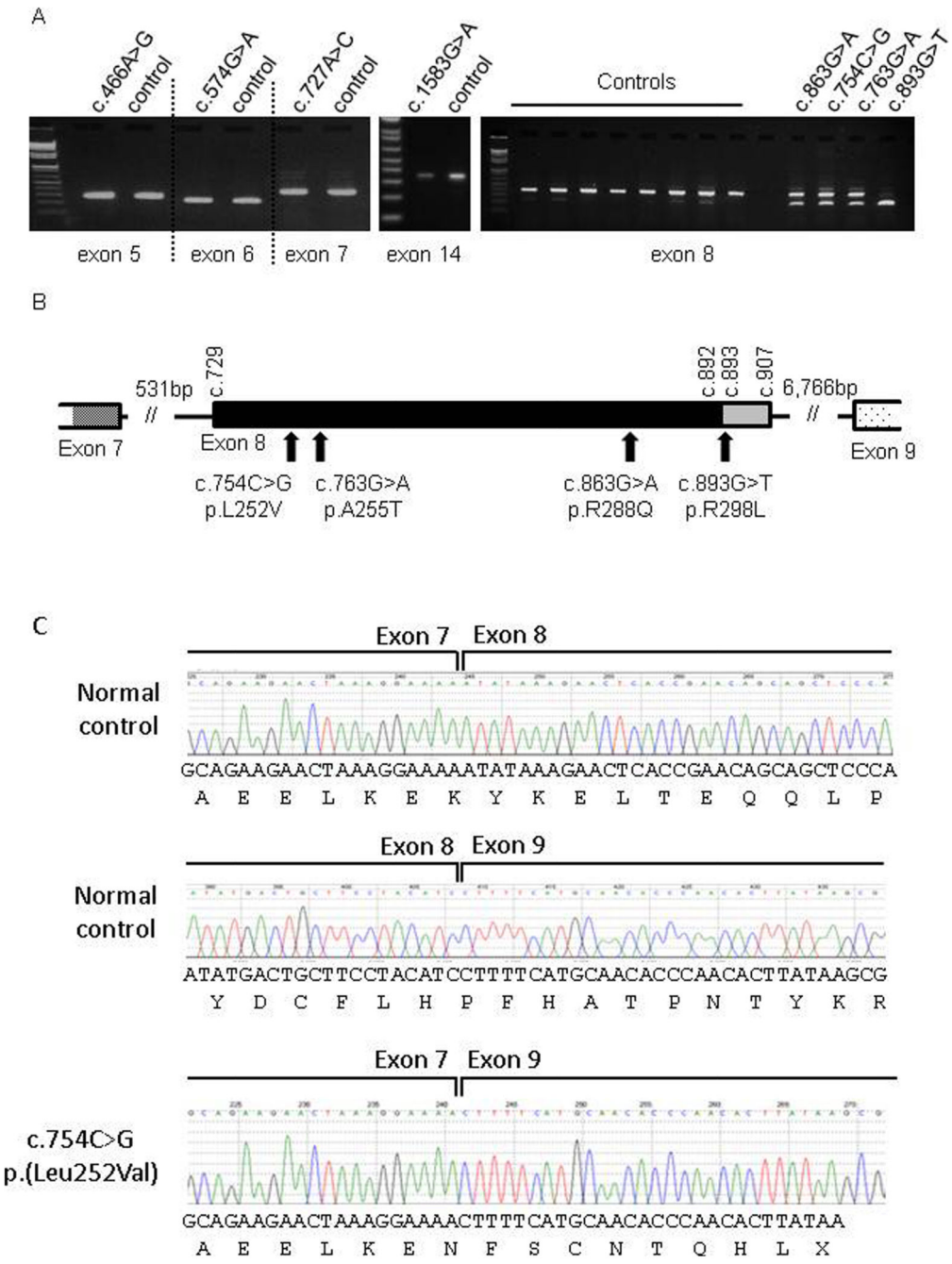

Figure 4.

Effect of exonic variants on exon skipping. (A) RT-PCR analysis using flanking primers, e.g. exon 5 was amplified using primers in exons 4 and 6. Exon skipping was seen with variants in exon 8 but not with variants in exons 5, 6, 7 or 14. Controls are patients with myeloid neoplasms without an EZH2 mutation in the relevant exon (B) The structure of exon 8 and location of variants. The 3' 15 bp alternatively spliced end of exon 8 is shown in grey. (C) Sequence traces of normal splicing between exons 7 and 8, and exon 8 (shorter exon variant)

Europe PMC Funders Author Manuscripts

and 9 (upper two traces) and result of skipping of exon 8 (lower trace) resulting in an out-of-frame transcript and a predicted p.(K243Nfs*10) truncated protein.

Europe PMC Funders Author Manuscripts

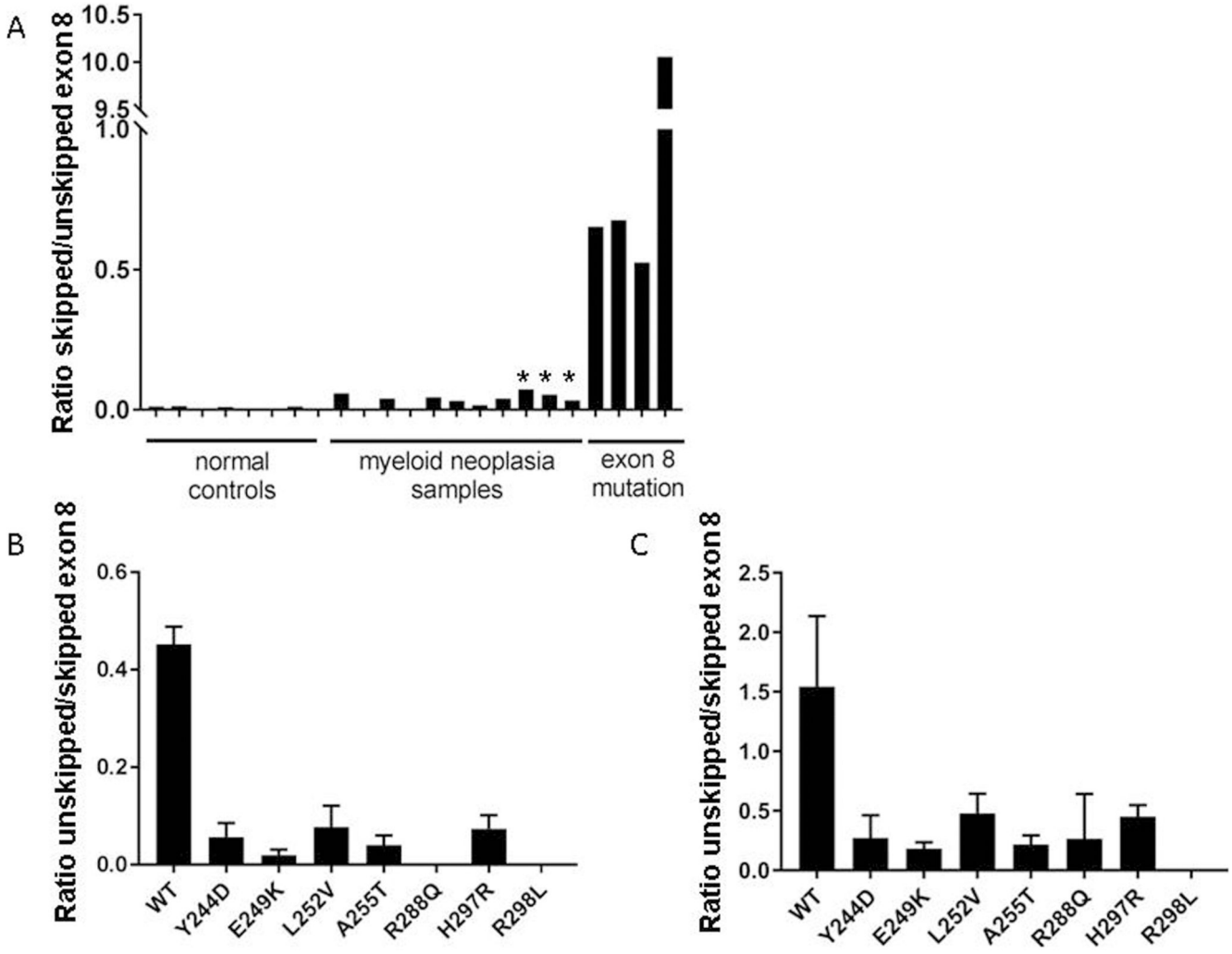

Figure 5.

(A) Exon 8 skipping in four *EZH2* exon 8 mutated samples, myeloid neoplasia samples without *EZH2* mutations, and healthy controls, as detected by FAM-labelled PCR and Genescan analysis. Myeloid neoplasia samples without *EZH2* mutations were all analysed by the Illumina Trusight myeloid panel. Three samples, marked with an asterisk, had mutations in the splicing factors *SRSF2* (two samples) and *U2AF1* (one sample). The effect of exon 8 variants on skipping of exon 8 was assessed using the pSpliceExpress minigene system in HEK293F cells (B) and HeLa cells (C). All mutations examined showed increased skipping compared to wild type *EZH2*.

Table 1

EZH2 mutation details and assay results. Where there are potentially pathogenic changes to methylation activity or splicing, these are indicated in bold. Coding and protein sequences are numbered according to transcript NM_004456.

Variant No.	Variant	Exon	Region	In-vitro histone methylation assay	Cell-based H3K27 methylation assay	Splicing by RT-PCR	Splicing by mini-gene assay
1	c.384A>C p.(Leu128Phe)	5	DI	ND	**Inactive**	Normal	ND
2	c.394C>T p.(Pro132Ser)	5	DI	ND	**Inactive**	ND	ND
3	c.401T>A p.(Met134Lys)	5	DI	ND	**Inactive**	ND	ND
4	c.434T>G p.(Phe145Cys)	5	DI	Active	**Inactive**	ND	ND
5	c.466A>G p.(Lys156Glu)	5	DI	ND	**Reduced activity**	ND	ND
6	c.574G>A p.(Asp192Asn)	6	Between DI and DII	Active	Active	Normal	ND
7	c.727A>C p.(Lys243Gln)	7	DII	ND	ND	Normal	ND
8	c.730T>G p.(Tyr244Asp)	8	DII	Active	**Reduced activity**	ND	**Abnormal**
9	c.745G>A p.(Glu249Lys)	8	DII	ND	Active	ND	**Abnormal**
10	c.754C>G p.(Leu252Val)	8	DII	ND	Active	**Abnormal**	**Abnormal**
11	c.763G>A p.(Ala255Thr)	8	DII	ND	Active	**Abnormal**	**Abnormal**
12	c.863G>A p.(Arg288Gln)	8	DII	ND	Active	**Abnormal**	**Abnormal**
13	c.890A>G p.(His297Arg)	8	DII	ND	ND	ND	**Abnormal**
14	c.893G>T p.(Arg298Leu)	8	DII	ND	Active	**Abnormal**	**Abnormal**
15	c.1033G>A p.(Ala345Thr)	10	Between DII and CXC	ND	Active	ND	ND
16	c.1583G>A p.(Cys528Tyr)	14	CXC	ND	ND	Normal	ND
17	c.1728C>G p(Cys576Trp)	15	CXC	**Inactive** *1*	ND	ND	ND
18	c.2068C>T p.(Arg690Cys)	18	SET	**Inactive** *1*	**Inactive**	ND	ND
19	c.2191T>G p.(Tyr731Asp)	19	SET	**Inactive** *1*	**Inactive**	ND	ND

(1) Results published in Ernst et al (2010) Key: ND, not done.